

Diagnostics on MINI-C Electron Beam

An earlier note (VIEW 20, p.21) gave some typical electron beam shapes and intensities at the close-in sample testing position (2.6 cm beyond the anode foil). Radial beam profiles for this position and for a more distant position (5.1 cm beyond the anode foil) at which high speed photography is employed were given in a following paper (VIEW 21, p.). These are also reproduced in figure 1 of the present note.

Having now analysed some 200 shots or so on beryllium and carbon samples we feel it may be of some interest (particularly to potential or actual users of MINI-C and EROS) to show the histogram distributions of output voltages and beam energies for these shots. Peak output voltages were read from the oscilloscope traces and beam energies were measured calorimetrically from the temperature rises of the sample (1" in diameter) and the surrounding graphite guard-ring (2 $\frac{5}{8}$ " in diameter).

Figure 2 shows the histogram distributions of beam energy (i.e. heat content) for various charging voltages on the MARX generator. Figure 1 enables the data of figure 2 (in cal) to be converted to an equivalent intensity (in cal cm⁻²) at any point. Although our present data for the photography position (5.1 cm from the anode) is sparse in comparison with that for the close-in position (2.6 cm from anode), it can be seen that intensities are lower by approximately 20% at the bigger distance*. It can be further seen that there is roughly a factor of 7 in beam intensity between the lowest (20 kV) and highest (60 kV) firing levels of the MARX generator. For any given firing level the average shot-to-shot variation (F.W.H.M.) of beam intensity is about $\pm 20\%$ (the maximum variation on any shot being about twice this i.e. $\pm 40\%$ - 50%).

It should be noted that heat content of the beam at the 2.6 cm position (shown in figure 2) is some 17% less than the total beam energy generated in the anode cathode gap. As discussed in VIEW 20 this can be attributed to about 10% loss from the fringe areas of the beam falling outside the outer guard-ring block of the calorimeter, and to about 6% loss due to electron backscatter from the sample and guard-ring ($Z \sim 6$). In the case of a target sample of high atomic number (Z) backscatter is very much larger (see figure 4; $\sim 20\%$ - 60% between 1 and 2 MeV for tungsten, $Z = 74$). The energy that would be deposited in such a sample can be obtained from figure 2 by scaling downwards using the data of figure 4.

Figure 3 shows the distributions of peak output voltage for various charging voltages on the MARX generator. Shot-to-shot variation is here about $\pm 15\%$ (F.W.H.M.). Voltages in excess of about 2 MeV (charging voltages > 60 kV) are avoided, if possible, since it is

*Other data (not shown) indicate that at even larger distances of about 10 cm the intensities have fallen by approximately a factor 2 below those at 2.6 cm.

our experience that these contribute to premature breakdown of insulators etc.

Although the main function of the Monte Carlo code ZEBRA is to predict the way in which the absorbed energy is deposited with depth in a material a bonus piece of information given for each run is the number of electrons backscattered and their total energy. Although neither of these quantities is measured experimentally (nor directly needed) it is of some interest to see how the fractional energy backscattered varies with the voltage and angle of incidence of the electrons and with the atomic number of the target material. Figure 4 shows the computed fractional energy backscattered (i.e. "reflected") as a function of these three parameters. It is seen to be very dependent on angle of incidence at low atomic number (approximately a factor of 20 difference between 0° and 60° for carbon) and rather less dependent at high atomic number. Backscatter increases appreciably with atomic number (between one and two orders of magnitude, depending on angle, between carbon and tungsten) and decreases with increasing electron energy (by up to a factor of five between 0.7 and 5 MeV). All of these calculations were done using complex energy spectra typically like the one shown inset to figure 4. Spectra between 0.7 and 2 MeV (applicable to MINI-C) were computed from actual analysis of the voltage and current waveforms as described in earlier notes. Since no similar waveform analysis was available at higher energies, those at 3 and 5 MeV (applicable to EROS) were obtained by suitable scaling of their MINI-C counterparts at low voltage on the assumption that the spectrum shape stayed roughly the same.

P. Fieldhouse }
J. G. Locke } SNE
G. W. Sentence }
A. C. Simmons }

D. Large SSDM

30th April, 1970.

Fig. 1. Radial Profiles of MINI C Electron Beam at Various Nominal Beam Energies (2.6 cm from Anode)

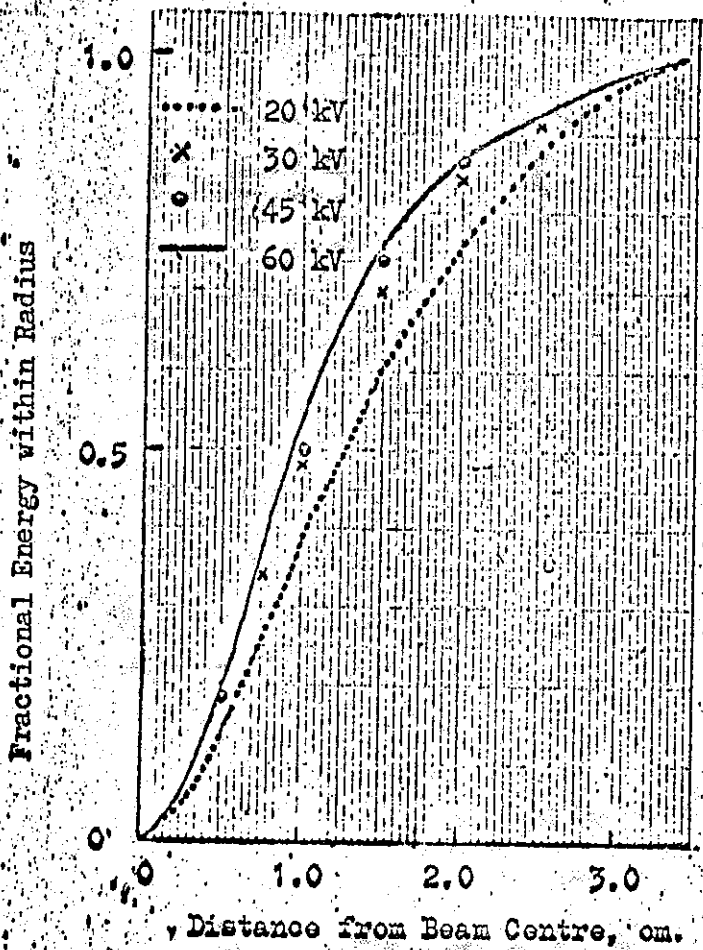
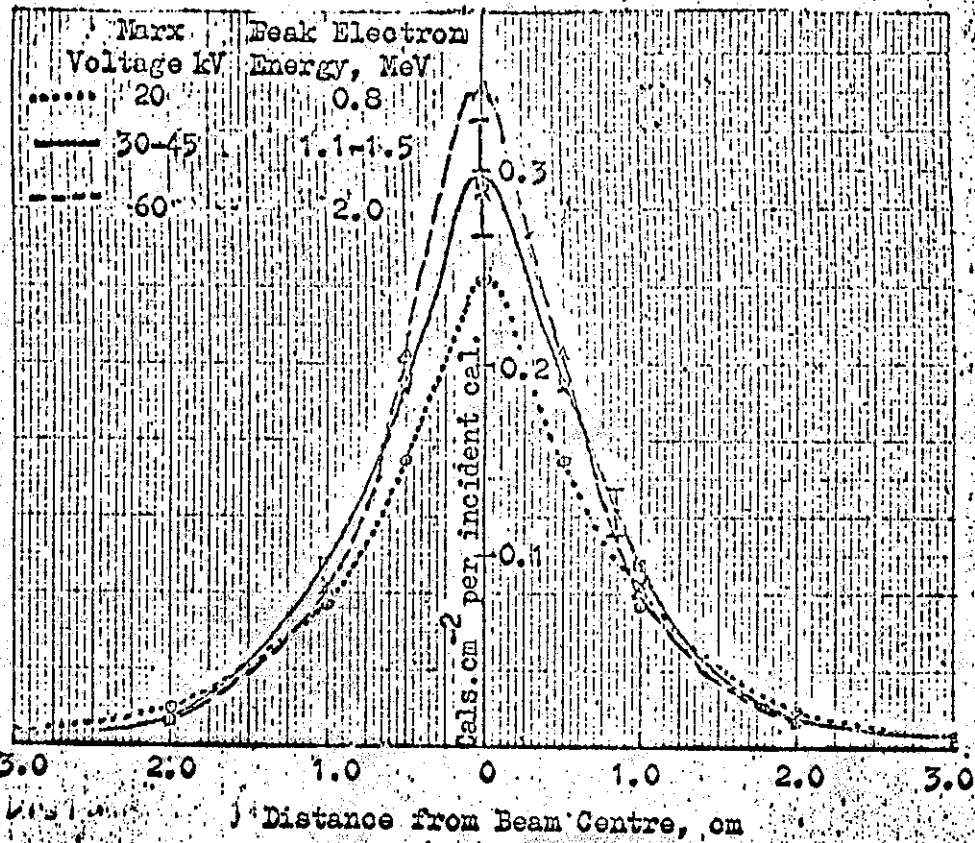
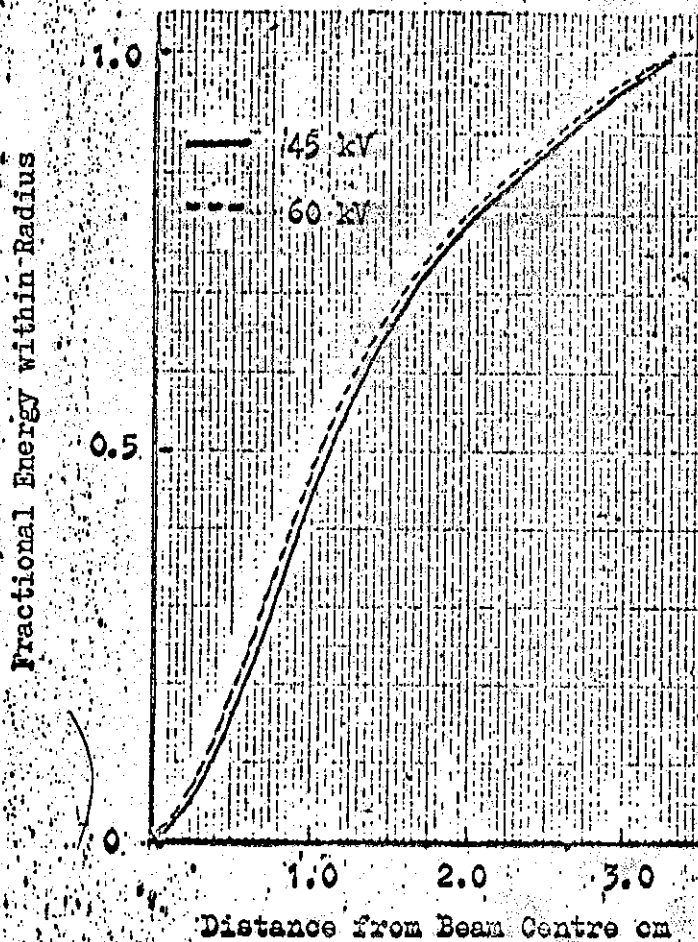
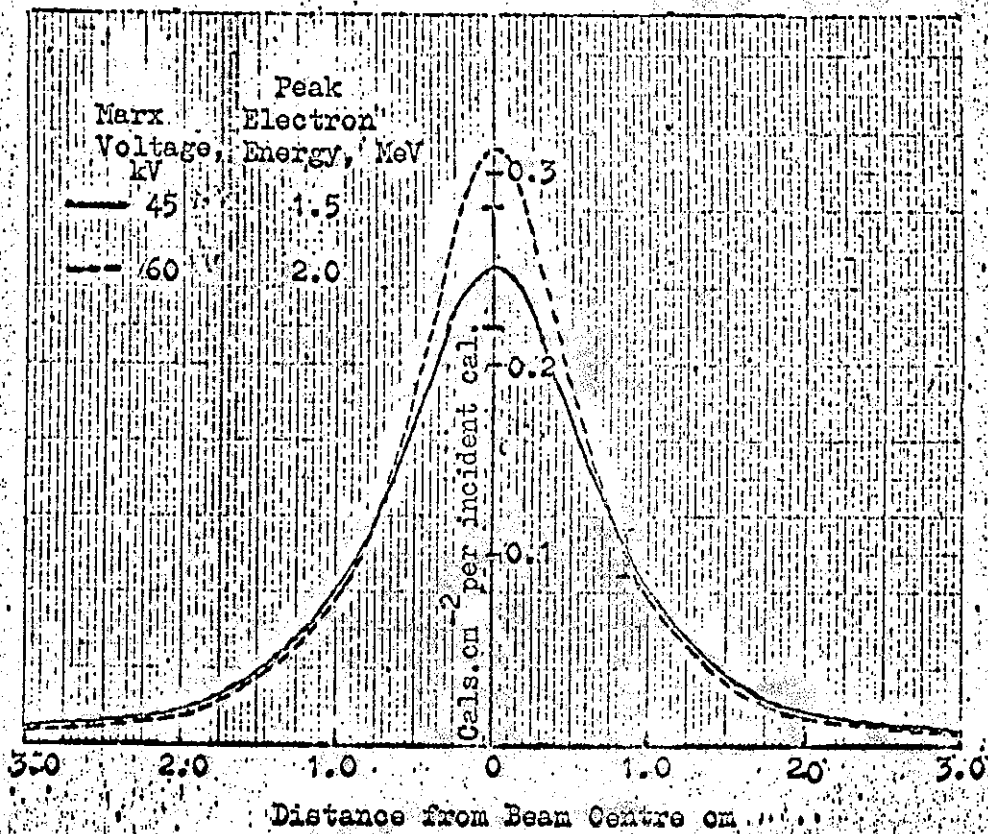


Fig. 1. Radial Profiles of MINI C Electron Beam at Various Nominal Beam Energies. (5.1 cm from Anode)



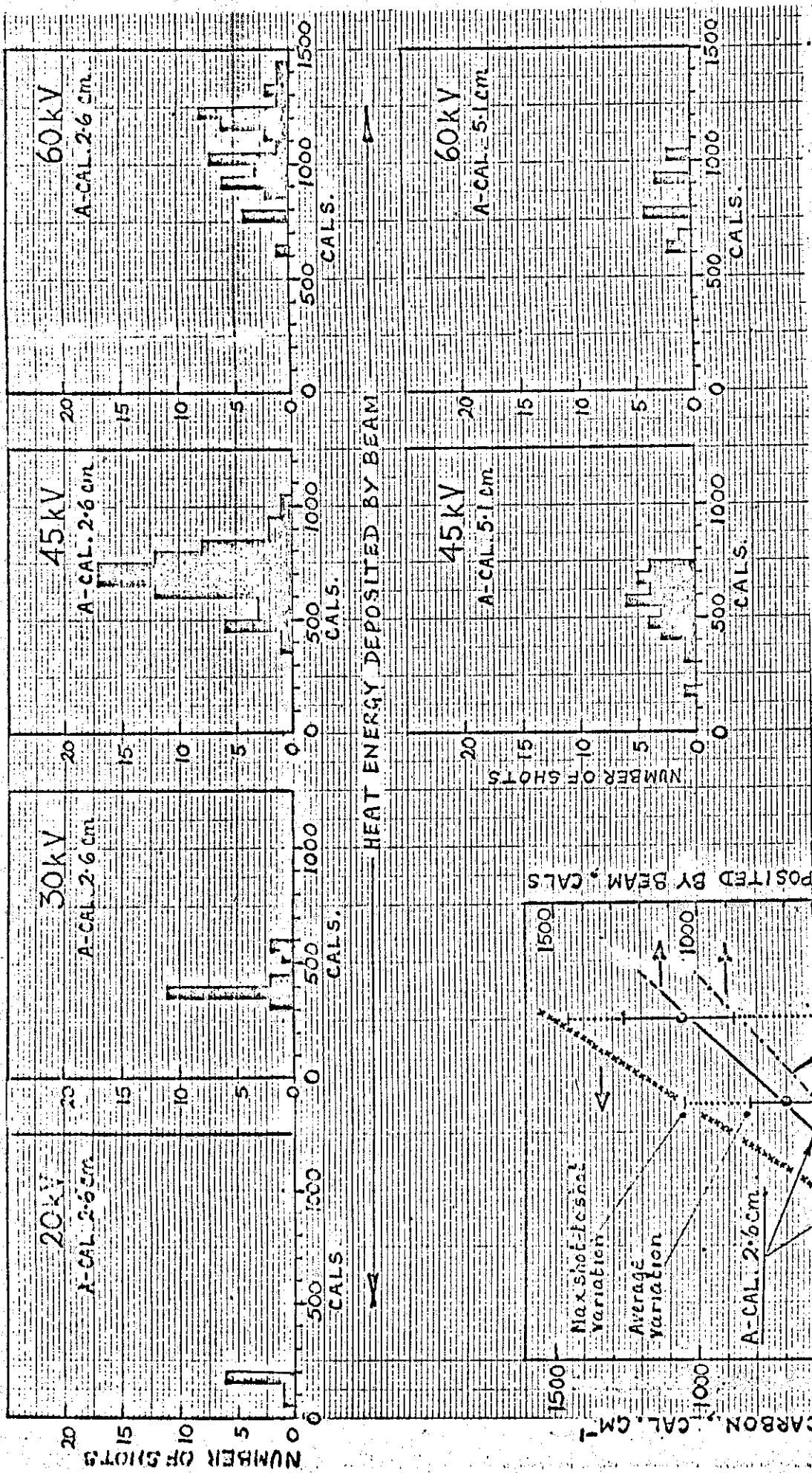
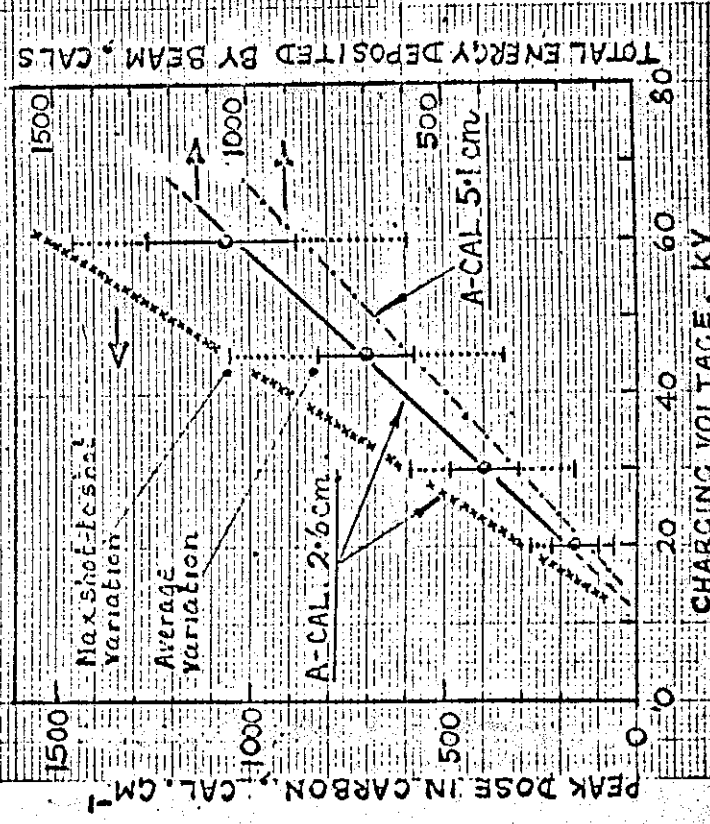


FIGURE 2 - HEAT ENERGY DEPOSITED IN A 2.5" DIAMETER CARBON CALORIMETER BY MINI-C ELECTRON BEAM (MARX charging voltages and anode foil-to-calorimeter distances are indicated in each case).



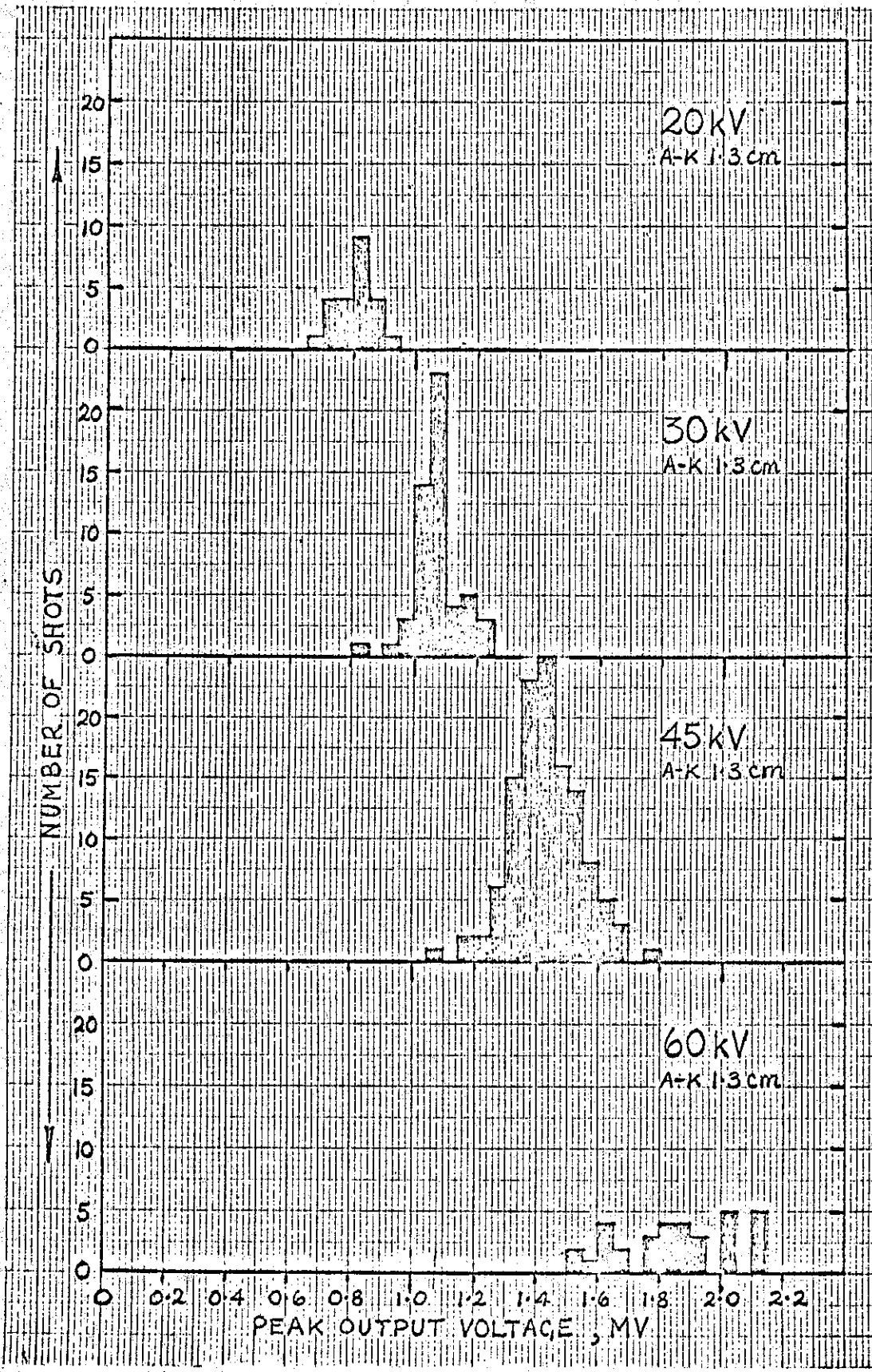
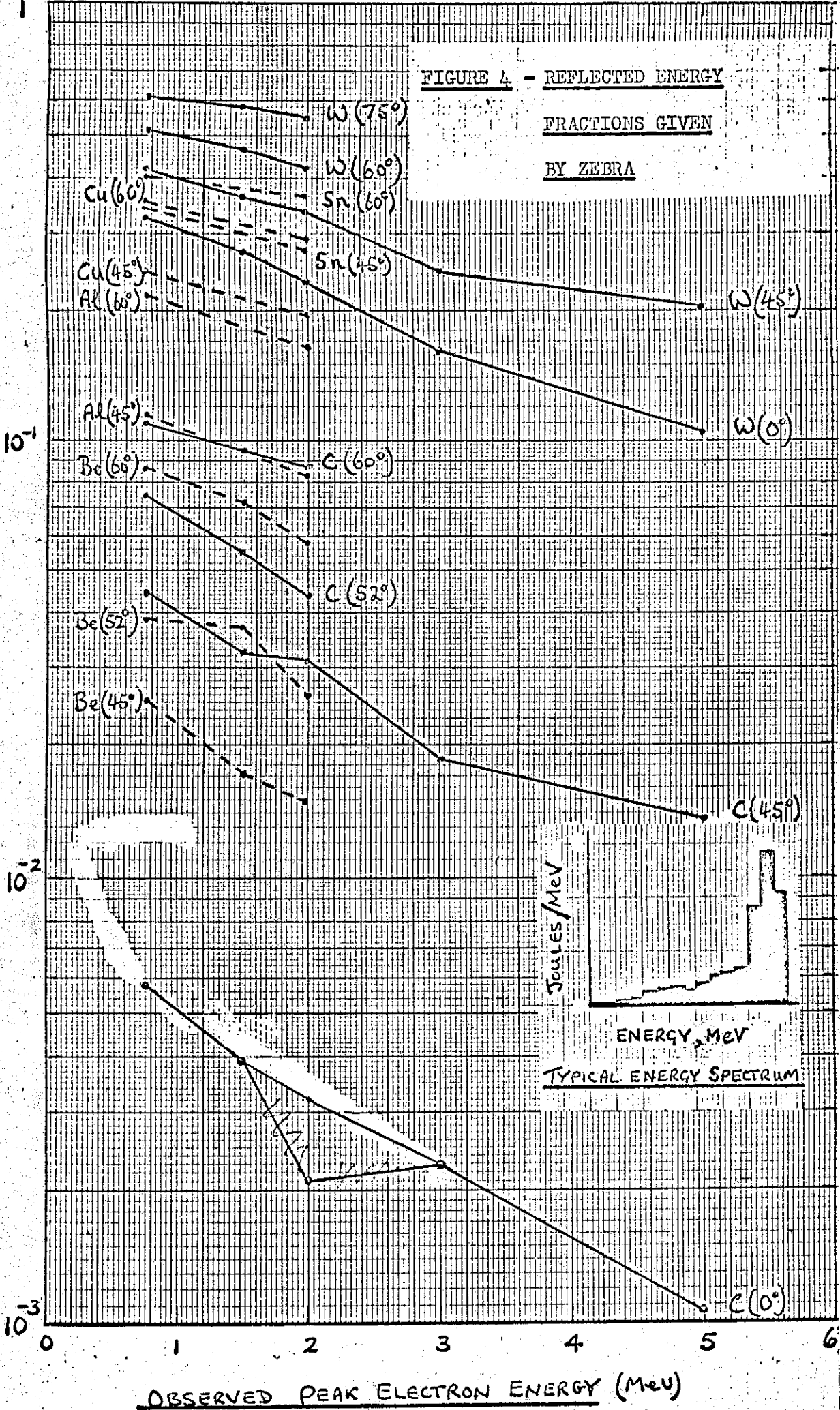


FIGURE 3 - DISTRIBUTION OF PEAK OUTPUT VOLTAGES OF MINI-C
 (MARX charging voltages and anode-to-cathode distances are indicated in each case).

FIGURE 4 - REFLECTED ENERGY
 FRACTIONS GIVEN
 BY ZEBRA

FRACTION OF ENERGY BACK SCATTERED



OBSERVED PEAK ELECTRON ENERGY (MeV)